Stabilizing a Platinum₁ Single-Atom Catalyst on Supported Phosphomolybdic Acid without Compromising Hydrogenation Activity

Bin Zhang, Hiroyuki Asakura, Jia Zhang, Jiaguang Zhang, Sudipta De, and Ning Yan*

Abstract: *In coordination chemistry, catalytically active metal complexes in a zero- or low-valent state often adopt four-coordinate square-planar or tetrahedral geometry. By applying this principle, we have developed a stable Pt_1 single-atom catalyst with a high Pt loading (close to 1 wt %) on phospho-molybdic acid(PMA)-modified active carbon. This was achieved by anchoring Pt on the four-fold hollow sites on PMA. Each Pt atom is stabilized by four oxygen atoms in a distorted square-planar geometry, with Pt slightly protruding from the oxygen planar surface. Pt is positively charged, absorbs hydrogen easily, and exhibits excellent performance in the hydrogenation of nitrobenzene and cyclohexanone. It is likely that the system described here can be extended to a number of stable SACs with superior catalytic activities.*

Single-atom catalysts (SACs), a class of catalysts where bare metal atoms are atomically dispersed or anchored on the support, are a new frontier in heterogeneous catalysis.[1] However, a key challenge that is often encountered is stabilization of isolated metals on a support without compromising catalytic activity. As the surface energy of single metal atoms is higher than corresponding metal clusters and nanoparticles, the atoms are highly mobile and tend to form aggregates during synthetic procedures.[2] Keeping the metal loading at a very low level to minimize agglomeration is a common practice employed to tackle the problem.[3] Another strategy is to anchor single atoms on a support with a stronger metal-support interaction.[4] Nevertheless, it remains difficult to effectively stabilize isolated atoms at increased metal loading, which hinders the viability of SACs in applications.

In classical coordination chemistry, catalytically active, stable complexes involving zero- or low-valent noble metals with single atomic identity are commonplace.[5] A close inspection of these compounds reveals that many of them are four-coordinate complexes containing a metal with a square-planar or tetrahedral coordination geometry, states that are intrinsically more stable. Inspired by this, we envisioned construction or introduction of four-coordinate anchoring sites with suitable geometry, thereby achieving a high loading of stable SACs on a support. Phosphomolybdic acid ($H_3PMo_{12}O_{40}$, PMA) was selected to examine the feasibility of the approach. PMA has a classical Keggin structure with one P atom in the center that is caged by 12 octahedral MoO_6-units linked together by 24 bridging oxygen atoms (O_{br}). Another 12 corner oxygen atoms (O_c) complete the structure, each of which is double-bonded with an additional Mo atom. With 36 oxygen atoms exposed, PMA furnishes a range of coordination sites (Figure 1), including the single corner site, the bridge site (the O_c-O_{br}-bridge site), the three-fold hollow site (3-H_O_c and 3-H_O_{br}), and the four-fold hollow site (4-H). Thus, PMA is an ideal material with which to differentiate the SACs stabilizing ability of various sites. Previously, several mononuclear organometallic compounds were loaded onto heteropolyacid-modified supports and used as anchored homogeneous catalysts for enantioselective hydrogenation.[6] Studies in which inorganic metal salts or organometallic complexes are anchored to prepare small metal nanoparticles and nanoclusters (2–4 nm) are also described.[7] To our knowledge, there have been no reports on highly active SACs on phosphomolybdic acid where the accurate location and electronic state of reduced single metal atoms has been determined.
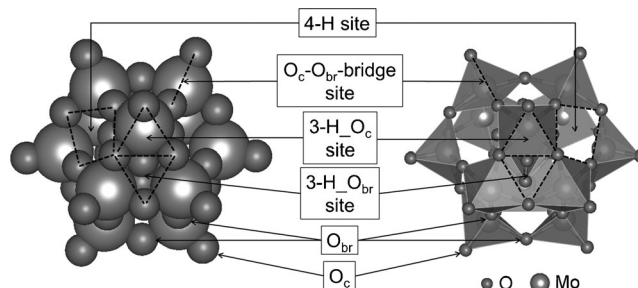
[*] B. Zhang, Dr. J. Zhang, Dr. S. De, Prof. Dr. N. Yan
     Department of Chemical and Biomolecular Engineering, National
     University of Singapore, 4 Engineering Drive 4
     Singapore 117585 (Singapore)
     E-mail: ning.yan@nus.edu.sg

     Dr. H. Asakura
     Department of Molecular Engineering, Graduate School of Engi-
     neering; Japan and Elements Strategy Initiative for Catalysts &
     Batteries (ESICB), Kyoto University, Kyotodaigaku Katsura
     Nishikyo-ku, Kyoto 615-8510; 615-8245 (Japan)

     Dr. J. Zhang
     Institute of High Performance Computing; Agency for Science,
     Technology and Research, 1 Fusionopolis Way #16-16 Connexis
     Singapore 138632 (Singapore)

Figure 1. Different types of surface O atoms and possible anchoring sites for Pt atoms on Keggin-structured anion phosphomolybdic acid ($PMo_{12}O_{40}{}^{3-}$). The P atom in the center is hidden inside the outer sphere O and Mo atoms.

The catalyst was synthesized by a simple three-step method. PMA was first embedded on a support by wet-impregnation. The primary screening of supports and solvents was based on the ability of the support to adsorb PMA at room temperature. A series of common supports (Al_2O_3, SiO_2, TiO_2, WO_3, ZSM-5, HY, HAP, $CaSiO_3$, and activated carbon (AC)) and solvents (H_2O, HCl in H_2O (0.5 M), ethanol, and acetone) were examined. AC exhibited the strongest affinity for PMA, resulting in 100% absorption regardless of the solvent. The exceptional affinity of AC for PMA can be attributed to its oxygen enriched hydroxyl, ketone, and carboxyl groups on the surface (Supporting Information, Figure S1 (XPS spectra) and Table S1 (elemental analysis)). Acetone was employed as the solvent, as PMA decomposes easily in water at elevated pH[8] and can oxidize alcohols. In the second step, readily reducible $Pt(acac)_2$ was introduced onto PMA/AC by impregnation. $Pt(acac)_2$ shares a similar size with PMA (0.7 nm vs. 1.0 nm) so that a 1:1 interaction between the precursor and the anchoring site is expected. Electrospray ionization mass spectrometry (ESI-MS) confirmed that $Pt(acac)_2$ was physically adsorbed on PMA, rather than undergoing proton exchange between ligands (Supporting Information, Figures S2 and S3). Following a final reduction step, Pt_1 SAC forms on PMA modified AC. We envisaged that our system could stabilize a large number of Pt single atoms: 1) Pt has a choice among various sites on PMA and may thus occupy the most stable configuration (thermodynamic control), and 2) the kinetic barrier of agglomeration for atoms anchored on spatially separated PMA species is substantially higher than those on unmodified support (kinetic control).

The reduction behavior of Pt pre-catalysts over H_2 was determined from their temperature-programmed reduction (TPR) profiles, as shown in Figure 2a. Unreduced sample is denoted as $Pt(acac)_2$-PMA/AC, and reduced sample as Pt-PMA/AC. For comparison, 1 wt% Pt on AC without PMA (denoted as $Pt(acac)_2$/AC before reduction, and Pt/AC after reduction, respectively) and PMA/AC were prepared following the same method. A reduction peak located at approximately 150°C was observed for $Pt(acac)_2$/AC, while the peak shifted to about 120°C for $Pt(acac)_2$-PMA/AC, indicating a change in the reducibility of $Pt(acac)_2$. Based on TPR profiles, 170°C was selected as the unified reducing temperature for all samples. After reduction, inductively coupled plasma optical emission spectrometry (ICP-OES) analysis indicated a Pt loading of 0.88 wt% on Pt/AC and 0.91 wt% on Pt-PMA/AC. FTIR spectra of reduced samples suggested complete removal of acac⁻ ligand (Supporting Information, Figures S4 and S5).

The reduced samples were then investigated by transmission electron microscopy (TEM) and powder X-ray diffraction (XRD) to probe the size and morphology of Pt species. As expected, no PMA aggregates were detected from TEM images in PMA/AC, suggesting uniform dispersion of PMA on AC (Supporting Information, Figure S6). Pt NPs in the size range of 1.7–3.6 nm (with an average of 2.5 nm) were observed in Pt/AC (Figure 2c; Supporting Information, Figure S7), whereas no NPs or clusters were detected on Pt-PMA/AC (Figure 2d). Nevertheless, energy-dispersive
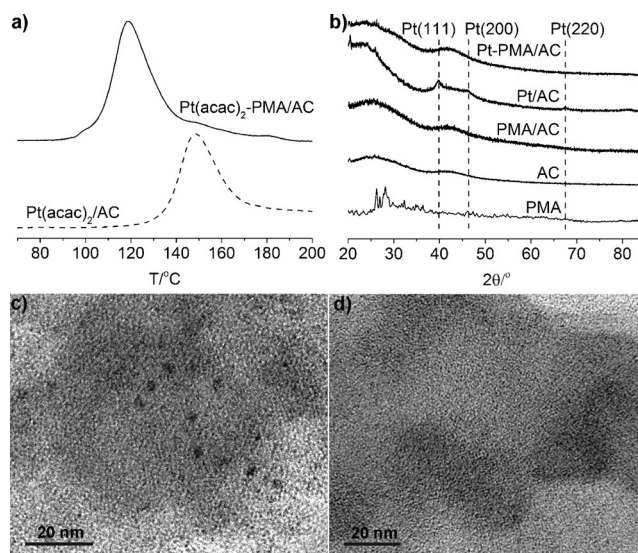

Figure 2. a) TPR profiles of $Pt(acac)_2$/AC and $Pt(acac)_2$-PMA/AC. Reduction conditions: 5% H_2 in N_2, 100 mL min⁻¹, 10°C min⁻¹ heating rate (70–200°C), catalyst (50 mg). Before heating, the sample was stabilized in 5% H_2 in N_2 at 70°C for 60 min. b) XRD patterns of PMA, AC, PMA/AC, Pt/AC, and Pt-PMA/AC. The predicted diffraction peaks for Pt metal are indicated with dashed lines. A typical TEM image of c) Pt/AC and d) Pt-PMA/AC.

X-ray spectroscopy (EDX) analysis of the same area on the Pt-PMA/AC material (Supporting Information, Figure S8) confirmed the existence of Pt with an estimated content of 0.97 wt%, very close to the ICP-OES results. In the XRD pattern of Pt/AC (Figure 2b), three peaks at 40°, 47°, and 68°, were observed, corresponding to the respective (111), (200), and (220) crystal phases of Pt NPs.[9] A crystallite size of 3.8 nm was estimated from the broadening profile of the (111) peak at 40° using the Scherrer equation. In contrast, no XRD peak was observed for Pt-PMA/AC. As such, the size of Pt species in Pt-PMA/AC is below the detection limit of XRD and TEM, possibly in the single-atom regime.

Extended X-ray absorption fine structure spectroscopy (EXAFS) provided key evidences on the dispersion of Pt species on PMA modified AC. A Pt-Pt contribution at about 2.7 Å was not observable in the k^3-weighted EXAFS at the Pt L_3-edge of Pt-PMA/AC (Figure 3a), strongly indicating that Pt exists predominantly as isolated atoms. The only prominent shell, located at approximately 1.8 Å, arises from a Pt-O contribution. Unlike Pt-PMA/AC, Pt/AC exhibited a strong Pt-Pt shell corroborating the existence of Pt NPs. A Pt-O shell was also detected, plausibly arising from the interactions between Pt NPs and the abundant surface oxygen-containing groups on AC. The spectrum of $Pt(acac)_2$-PMA/AC strongly resembled that of pure $Pt(acac)_2$, in good agreement with ESI-MS analysis, where only a weak interaction between $Pt(acac)_2$ and PMA was identified. Combining TEM, XRD, and in particular EXAFS analysis, it is evident that Pt SACs could be successfully obtained on PMA modified AC with a loading close to 1 wt%.

Curve-fitting was conducted based on two main peaks in the R range of 1–3.2 Å. The resulting first shell coordination parameters, bond length, and the corresponding standard
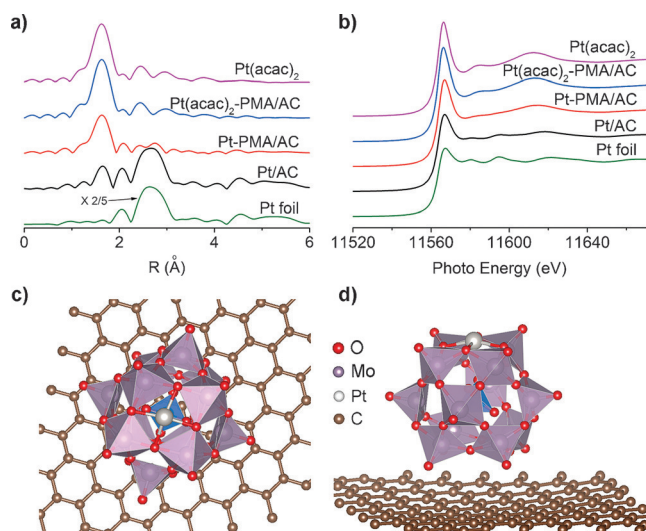
Figure 3. a) The k^3-weighted Fourier transform spectra derived from EXAFS for AC-supported Pt catalysts and precatalyst, Pt(acac)$_2$, and Pt foil; $\Delta k = 3.0–13.0$ Å^{-1}. b) Normalized XANES spectra at the Pt L$_3$-edge of AC-supported Pt catalysts and precatalyst, Pt(acac)$_2$, and Pt foil. The spectra exhibited a decreasing trend in the intensities of white-line: Pt(acac)$_2$ (1.65) ≈ Pt(acac)$_2$-PMA/AC (1.66) > Pt-PMA/AC (1.53) > Pt/AC (1.36) > Pt foil (1.20). The numbers in parentheses refer to the normalized absorption height for different samples. c) Top view and d) side view of the most stable configuration of Pt$_1$ on PMA/graphene, based on DFT calculations.

deviations are summarized in Table S5 (Supporting Information). As expected, a Pt-O coordination number of around four was found for both Pt(acac)$_2$ and Pt(acac)$_2$-PMA/AC samples. Meanwhile, the Pt-O coordination number remained 3.4 in Pt-PMA/AC, although all oxygen-containing ligands were removed during reduction. Considering the fitting error of XAFS analysis (ca. 20%), the Pt-O coordination number can be either three or four. To understand the exact bonding state of Pt on PMA/AC, DFT calculations were carried out to investigate the adsorption behavior of Pt atoms on the PMA system. A graphene layer was used as the support in the modelling because it possesses a simple and unified structure (see the Supporting Information, Figure S9 for the optimized geometry of PMA on the support). Subsequently, four sites were considered for Pt adsorption, including the four-fold hollow site (4-H), the three-fold hollow site surrounded by three O$_{br}$ atoms (3-H_O$_{br}$), the three-fold hollow site formed by one O$_c$ atom and two O$_{br}$ atoms (3-H_O$_c$), as well as the O$_c$-O$_{br}$ bridge site (Figure 3c,d; Supporting Information, Figure S10). The structures were fully optimized, revealing that the Pt atom does indeed prefer to adsorb on the four-fold hollow site with an adsorption energy of −5.72 eV. In this coordination mode, Pt and surrounding O atoms adopt quasi square-planar geometry, with Pt−O bond lengths ranging from 2.00 to 2.02 Å. The Pt atom protrudes slightly from the oxygen planar surface. It is interesting to note that three-fold hollow sites were not stable for Pt adsorption. After full structural relaxation, Pt atoms move from the initial site to the O$_{br}$-O$_{br}$_bridge site with a Pt−O bond length of 1.95 Å. The adsorption energies may be ranked in increasing order: four-fold hollow site (−5.72 eV) < three-fold hollow sites

(move to O$_{br}$-O$_{br}$ bridge site, −3.94 eV) < O$_c$-O$_{br}$ bridge site (−3.56 eV). Considering the fitted coordination number and DFT calculation results, we propose that each Pt atom interacts with four bridging oxygen atoms in the four-fold hollow site on PMA to form a relatively stable structure (Figure 3c,d). This coordination mode satisfies the empirical requirements of coordination chemistry, which supports stable zero- or low-valent Pt, and therefore explains the capability of the system to support a high loading of Pt single atoms without agglomeration.

The electronic interactions between reduced Pt single atoms and PMA were investigated by X-ray absorption near-edge structure (XANES) analysis. The Pt white-line intensity for Pt/AC at 11 568 eV[3a] is similar to Pt foil (Figure 3b). In contrast, the white-line intensity of Pt-PMA/AC is considerably higher than that of Pt foil, but lower than that of Pt(acac)$_2$ and Pt(acac)$_2$-PMA/AC. This observation confirms that Pt species in Pt-PMA/AC are positively charged by charge transfer from Pt to PMA (even after reduction), in excellent agreement with the coordination mode suggested by XAFS analysis and DFT calculations, where one Pt atom is coordinated by several oxygen atoms. Additional evidence of Pt-PMA interaction was obtained by XPS analysis. In the Mo 3d XPS spectrum of Pt-PMA/AC (Supporting Information, Figure S12d), the binding energy of Mo slightly decreased after reduction, indicating an increase of electron density in the presence of Pt. The ^{31}P MAS NMR spectra of PMA/AC and Pt-PMA/AC (Supporting Information, Figure S13) display signals at −2.7 and −6.2 ppm, respectively, suggesting an appreciable change of the electronic environment of P. The NH$_3$ desorption peak in temperature-programmed desorption (TPD) curves shifted from about 390 °C on PMA/AC to approximately 340 °C on Pt-PMA/AC, implying that the PMA decreased in acidity upon interaction with Pt (Supporting Information, Figure S14). Moreover, Bader charge[10] calculations indicate that the Pt atom loses 0.83 |e| at the four-fold hollow site. On this basis, coordination of Pt by oxygen resulted in an electron flow from Pt to PMA, producing stable, positively charged Pt single atoms.

To study the surface dispersion of Pt atoms, H$_2$-O$_2$ titration was applied, involving treatment of the freshly reduced samples with air, followed by titration with H$_2$. This method was utilized instead of direct H$_2$ titration, mainly to avoid occupation of Pt atoms by H atoms introduced by H$_2$/N$_2$ reduction, which cannot be completely removed below about 400 °C.[11] Control experiments showed that neither AC nor PMA/AC could absorb H$_2$ (Supporting Information, Figure S15), suggesting that any H$_2$ uptake is due to the presence of Pt. During titration, Pt/AC was saturated with H$_2$ after only two pulses, whereas Pt-PMA/AC (with the same Pt content) was able to consume H$_2$ equivalent to five pulses, demonstrating a much higher percentage of exposed Pt atoms on the latter material (Figure 4a,b). Indeed, the Pt dispersion on Pt-PMA/AC was calculated as 86%, not far from the predicted value of 100% for SACs. In comparison, the Pt dispersion on Pt/AC was only 24%, which is a typical value for supported Pt nanoparticles several nanometers in size (Supporting Information, Table S6). The H$_2$-O$_2$ titration experiment demonstrated the excellent hydrogen absorption
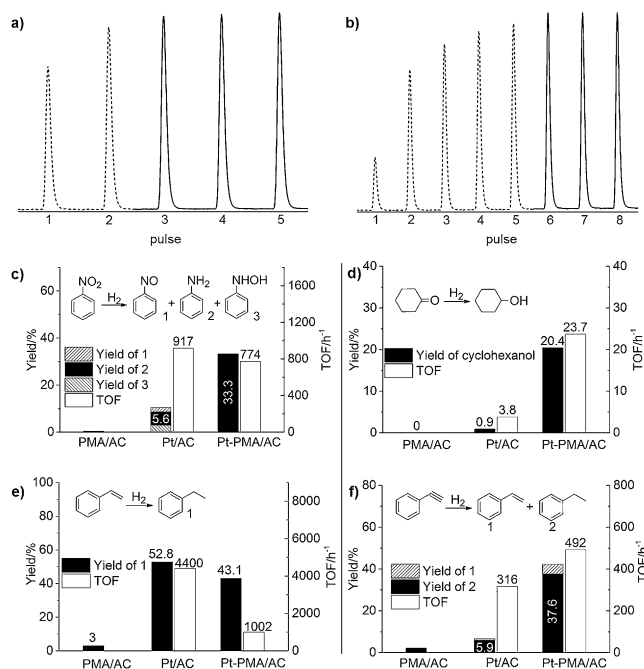
Figure 4. H₂ pulse titration profiles of samples after treatment with air: a) Pt/AC, b) Pt-PMA/AC. Titration conditions: N₂-carrier gas, 100 mL min⁻¹; 100 °C; H₂-titration gas, 159 µL/pulse; catalyst (120 mg). Before titration the sample was treated in air at 100 °C for 30 min. c–f) Catalytic performance of PMA/AC, Pt/AC, and Pt-PMA/AC in hydrogenation reactions. Reaction conditions: catalyst (5 mg), 1.0 MPa H₂ (2.0 MPa for cyclohexanone), ethyl acetate (2 mL), 1 h, room temperature (50 °C for cyclohexanone). For (c) nitrobenzene (53.6 µL), Pt:nitrobenzene = 1:2000 (mol mol⁻¹); for (d) cyclohexanone (2.7 µL), Pt:cyclohexanone = 1:100 (mol mol⁻¹); for (e) styrene (57.3 µL), Pt:styrene = 1:2000 (mol mol⁻¹); for (f) phenylacetylene (27.4 µL), Pt:phenylacetylene = 1:1000 (mol mol⁻¹).

property of Pt-PMA/AC, implying that the material has potential in hydrogenation reactions.

Consequently, hydrogenations of -NO₂, -C=O, -C=C and -C≡C groups were conducted. Initially, catalytic hydrogenation of nitrobenzene was performed under mild conditions, given that substantial activity was previously observed on Pt SACs supported on FeOₓ.[12] Nitrobenzene conversion was maintained below 30 % in all cases to ensure that the reaction remained under kinetic control. Little product was detected in Pt-free (Figure 4c), Pt(acac)₂-PMA/AC, or Pt(acac)₂ control catalysts (Supporting Information, Table S7, Entry 1,2), but both Pt/AC and Pt-PMA/AC were very active. Although the estimated TOFs for the two catalysts were comparable (ca. 900 h⁻¹ for Pt/AC, ca. 800 h⁻¹ for Pt-PMA/AC; calibrated by Pt dispersion), drastically different product distributions were observed. Over Pt/AC, five different products were detected, including aniline, nitrosobenzene, phenylhydroxylamine, azo-benzene, and azoxybenzene; the overall selectivity towards aniline was only 50 %. In sharp contrast, aniline was the only product obtained over Pt-PMA/AC. Considering that the side products are all intermediates in nitrobenzene hydrogenation, the exceptional selectivity may, at least partially, be due to the presence of Pt single atoms on the PMA-modified catalyst, which adsorb and polarize the intermediates and transform them into aniline. Recycling of Pt-PMA/AC was performed, and the catalyst exhibited high activity and excellent selectivity over five cycles (Supporting Information, Figure S17). Longer term stability of Pt-PMA/AC was also tested with a nitrobenzene:Pt ratio of 8000:1. The catalyst maintained an average TOF of about 800 h⁻¹, enabling quantitative substrate conversion in 10 h.

Subsequently, we extended the application of Pt SACs to the hydrogenation of the -C=O group in cyclohexanone (Figure 4 d). Pt-PMA/AC exhibited a TOF six times higher than that of Pt/AC under the same conditions, confirming that the positively charged, four-oxygen coordinated single Pt atoms on Pt-PMA/AC are superior active sites when it comes to activating polar functional groups. As we are aware, this is the first example where SACs are reported with a significantly higher activity in carbonyl group hydrogenation compared to non-SACs with a similar metal loading. Pt-PMA/AC was also more active than Pt/AC in the hydrogenation of phenyl-acetylene (Figure 4 f), but it was less effective in C=C bond hydrogenation (Figure 4 e). The difference in catalytic activity could be rationalized by different substrate adsorptions, as well as different hydrogen activation on Pt NPs and on isolated, charged Pt atoms. It is worth mentioning that PMA may not be an "innocent" support for catalysis because of its acidic nature. 3 wt % and 10 wt % PMA were intentionally added on Pt/AC; the latter induced complete deactivation of Pt/AC, whereas the former increased selectivity in nitro-benzene hydrogenation, although with reduced activity (Supporting Information, Tables S7–S10).

The catalytic mechanisms operating over Pt-PMA/AC and Pt/AC could be fundamentally different. On Pt/AC, hydrogen and substrate activation are achieved on a NP surface, followed by surface reaction among adsorbed species. On the contrary, both hydrogen and substrate activation occur on a single Pt atom on Pt-PMA/AC. Based on DFT calculations, the substrate adsorption pulls the Pt atom away from the most stable 4-H site (coordination number four) to an off-4-H site leading to reduced oxygen coordination, but the total coordination number remains four (Supporting Information, Table S11 and Figure S18b–e). Co-adsorption of hydrogen and cyclohexanone resulted in a much higher adsorption energy (−2.96 eV) than that for pure cyclohexanone adsorption (−0.50 eV), suggesting the feasibility of a co-adsorption strategy (Supporting Information, Table S11 and Figure S18 f). Interestingly, removing the adsorbed molecules and fully optimizing the structure caused the Pt atom to shift from the off-4-H site back to the four-coordinate 4-H site, thereby recovering the catalyst. This mechanism is consistent with a recent study, where single Pt atoms coordinated with four sulfur atoms in the resting state, but only coordinated with two sulfur atoms during the catalytic cycle.[13] A detailed kinetic study, in situ spectro-scopic analysis, and DFT calculations are needed to reveal the exact working mechanism of the Pt-PMA/AC catalyst, and to establish the concrete role of PMA in the reaction.

In summary, we have shown that a high loading of atomically dispersed Pt catalyst is achieved by stabilizing Pt on PMA with a classical four-coordinate quasi square-planar geometry. The stability of Pt single atoms is promoted by an

enhanced kinetic barrier to agglomeration, which is due to the spatial separation of PMA species on the support. Anchored Pt atoms strongly interact with PMA, inducing an electron out-flow, and exhibiting remarkable catalytic performance in the hydrogenation of nitro and ketone substrates. The strategy presented highlights the potential for improvement to SACs by harnessing the propitious aspects of coordination chemistry and homogeneous catalysis. The approach may be extended to the preparation of a broad spectrum of high loading single-atom catalysts with different combinations of metals, anchoring reagents, and supports, with a wide range of catalytic applications.

[1] a) B. Qiao, A. Wang, X. Yang, L. F. Allard, Z. Jiang, Y. Cui, J. Liu, J. Li, T. Zhang, *Nat. Chem.* **2011**, *3*, 634–641; b) J. Thomas, Z. Saghi, P. Gai, *Top. Catal.* **2011**, *54*, 588–594; c) M. Flytzani-Stephanopoulos, B. C. Gates, *Annu. Rev. Chem. Biomol. Eng.* **2012**, *3*, 545–574; d) X.-F. Yang, A. Wang, B. Qiao, J. Li, J. Liu, T. Zhang, *Acc. Chem. Res.* **2013**, *46*, 1740–1748; e) S. Sun, G. Zhang, N. Gauquelin, N. Chen, J. Zhou, S. Yang, W. Chen, X. Meng, D. Geng, M. N. Banis, R. Li, S. Ye, S. Knights, G. A. Botton, T.-K. Sham, X. Sun, *Sci. Rep.* **2013**, *3*, 1775–1783; f) Z.-Y. Li, Z. Yuan, X.-N. Li, Y.-X. Zhao, S.-G. He, *J. Am. Chem. Soc.* **2014**, *136*, 14307–14313; g) J. M. Thomas, *Nature* **2015**, *525*, 325–326; h) H. Yan, H. Cheng, H. Yi, Y. Lin, T. Yao, C. Wang, J. Li, S. Wei, J. Lu, *J. Am. Chem. Soc.* **2015**, *137*, 10484–10487; i) S. Yang, J. Kim, Y. J. Tak, A. Soon, H. Lee, *Angew. Chem. Int. Ed.* **2016**, *55*, 2058–2062; *Angew. Chem.* **2016**, *128*, 2098–2102; j) Y. Chen, T. Kasama, Z. Huang, P. Hu, J. Chen, X. Liu, X. Tang, *Chem. Eur. J.* **2015**, *21*, 17397–17402; k) S. Liang, C. Hao, Y. Shi, *ChemCatChem* **2015**, *7*, 2559–2567.

[2] a) Y.-T. Kim, K. Ohshima, K. Higashimine, T. Uruga, M. Takata, H. Suematsu, T. Mitani, *Angew. Chem. Int. Ed.* **2006**, *45*, 407–411; *Angew. Chem.* **2006**, *118*, 421–425; b) A. Corma, P. Concepción, M. Boronat, M. J. Sabater, J. Navas, M. J. Yacaman, E. Larios, A. Posadas, M. A. López-Quintela, D. Buceta, E. Mendoza, G. Guilera, A. Mayoral, *Nat. Chem.* **2013**, *5*, 775–781; c) J. Xing, J. F. Chen, Y. H. Li, W. T. Yuan, Y. Zhou, L. R. Zheng, H. F. Wang, P. Hu, Y. Wang, H. J. Zhao, Y. Wang, H. G. Yang, *Chem. Eur. J.* **2014**, *20*, 2138–2144; d) K. Ding, A. Gulec, A. M. Johnson, N. M. Schweitzer, G. D. Stucky, L. D. Marks, P. C. Stair, *Science* **2015**, *350*, 189–192; e) T. E. James, S. L. Hemmingson, C. T. Campbell, *ACS Catal.* **2015**, *5*, 5673–5678.

[3] a) M. Moses-DeBusk, M. Yoon, L. F. Allard, D. R. Mullins, Z. Wu, X. Yang, G. Veith, G. M. Stocks, C. K. Narula, *J. Am. Chem. Soc.* **2013**, *135*, 12634–12645; b) L. Wang, S. Zhang, Y. Zhu, A. Patlolla, J. Shan, H. Yoshida, S. Takeda, A. I. Frenkel, F. Tao, *ACS Catal.* **2013**, *3*, 1011–1019; c) F. R. Lucci, J. Liu, M. D. Marcinkowski, M. Yang, L. F. Allard, M. Flytzani-Stephanopoulos, E. C. H. Sykes, *Nat. Commun.* **2015**, *6*, 8550; d) S. Zhang, L. Nguyen, J.-X. Liang, J. Shan, J. Liu, A. I. Frenkel, A. Patolla, W. Huang, J. Li, F. Tao, *Nat. Commun.* **2015**, *6*, 7938; e) A. Corma, O. G. Salnikov, D. A. Barskiy, K. V. Kovtunov, I. V. Koptyug, *Chem. Eur. J.* **2015**, *21*, 7012–7015.

[4] a) Z. Zhang, W. Tang, M. Neurock, J. T. Yates, *J. Phys. Chem. C* **2011**, *115*, 23848–23853; b) M. Yang, S. Li, Y. Wang, J. A. Herron, Y. Xu, L. F. Allard, S. Lee, J. Huang, M. Mavrikakis, M. Flytzani-Stephanopoulos, *Science* **2014**, *346*, 1498–1501; c) J. D. Kistler, N. Chotigkrai, P. Xu, B. Enderle, P. Praserthdam, C.-Y. Chen, N. D. Browning, B. C. Gates, *Angew. Chem. Int. Ed.* **2014**, *53*, 8904–8907; *Angew. Chem.* **2014**, *126*, 9050–9053; d) C. K. Narula, L. F. Allard, G. M. Stocks, M. Moses-DeBusk, *Sci. Rep.* **2014**, *4*, 7238–7243; e) G. Vilé, D. Albani, M. Nachtegaal, Z. Chen, D. Dontsova, M. Antonietti, N. López, J. Pérez-Ramírez, *Angew. Chem. Int. Ed.* **2015**, *54*, 11265–11269; *Angew. Chem.* **2015**, *127*, 11417–11422; f) D. Deng, X. Chen, L. Yu, X. Wu, Q. Liu, Y. Liu, H. Yang, H. Tian, Y. Hu, P. Du, R. Si, J. Wang, X. Cui, H. Li, J. Xiao, T. Xu, J. Deng, F. Yang, P. N. Duchesne, P. Zhang, J. Zhou, L. Sun, J. Li, X. Pan, X. Bao, *Sci. Adv.* **2015**, *1*, e1500462; g) F. Dvorak, M. Farnesi Camellone, A. Tovt, N.-D. Tran, F. R. Negreiros, M. Vorokhta, T. Skala, I. Matolinova, J. Myslivecek, V. Matolin, S. Fabris, *Nat. Commun.* **2016**, *7*, 10801; h) C. Wang, M. Yang, M. Flytzani-Stephanopoulos, *AIChE J.* **2016**, *62*, 429–439; i) Z. Chen, S. Pronkin, T.-P. Fellinger, K. Kailasam, G. Vilé, D. Albani, F. Krumeich, R. Leary, J. Barnard, J. M. Thomas, J. Pérez-Ramírez, M. Antonietti, D. Dontsova, *ACS Nano* **2016**, *10*, 3166–3175.

[5] G. W. F. Albert Cotton, C. A. Murillo, M. Bochmann, *Advanced Inorganic Chemistry*, 6th ed., Wiley, New York, **1999**.

[6] a) J. A. M. Brandts, P. H. Berben, *Org. Process Res. Dev.* **2003**, *7*, 393–398; b) M. Rosario Torviso, M. N. Blanco, C. V. Cáceres, J. M. Fraile, J. A. Mayoral, *J. Catal.* **2010**, *275*, 70–77; c) S. K. Tanielyan, R. L. Augustine, N. Marin, G. Alvez, *ACS Catal.* **2011**, *1*, 159–169; d) S.-H. Ahn, M.-S. Choi, J.-S. Im, R. Sheikh, Y.-H. Park, *J. Mol. Catal. A* **2013**, *373*, 55–60; e) S. Tanielyan, N. Biunno, R. Bhagat, R. Augustine, *Top. Catal.* **2014**, *57*, 1564–1569; f) P. He, B. Xu, X. Xu, L. Song, X. Wang, *Chem. Sci.* **2016**, *7*, 1011–1015.

[7] a) T. Maiyalagan, *Int. J. Hydrogen Energy* **2009**, *34*, 2874–2879; b) Y.-H. Chin, C. Buda, M. Neurock, E. Iglesia, *J. Am. Chem. Soc.* **2011**, *133*, 15958–15978; c) Z. Cui, P. J. Kulesza, C. M. Li, W. Xing, S. P. Jiang, *Int. J. Hydrogen Energy* **2011**, *36*, 8508–8517; d) J.-S. Li, H.-Q. Dong, S.-L. Li, R.-H. Li, Z.-H. Dai, J.-C. Bao, Y.-Q. Lan, *New J. Chem.* **2016**, *40*, 914–918.

[8] A. Jürgensen, J. B. Moffat, *Catal. Lett.* **1995**, *34*, 237–244.

[9] W. Zhang, J. Chen, A. I. Minett, G. F. Swiegers, C. O. Too, G. G. Wallace, *Chem. Commun.* **2010**, *46*, 4824–4826.

[10] G. Henkelman, A. Arnaldsson, H. Jónsson, *Comput. Mater. Sci.* **2006**, *36*, 354–360.

[11] J. R. Anderson, K. Foger, R. J. Breakspere, *J. Catal.* **1979**, *57*, 458–475.

[12] a) H. Wei, X. Liu, A. Wang, L. Zhang, B. Qiao, X. Yang, Y. Huang, S. Miao, J. Liu, T. Zhang, *Nat. Commun.* **2014**, *5*, 5634; b) G. Xu, H. Wei, Y. Ren, J. Yin, A. Wang, T. Zhang, *Green Chem.* **2016**, *18*, 1332–1338.

[13] C. H. Choi, M. Kim, H. C. Kwon, S. J. Cho, S. Yun, H.-T. Kim, K. J. J. Mayrhofer, H. Kim, M. Choi, *Nat. Commun.* **2016**, *7*, 10922.